

# DETECTION MODEL FOR EFFECT OF SOIL SALINITY AND TEMPERATURE ON FDR MOISTURE CONTENT SENSORS

B. Liu, W. T. Han, P. Weckler, W. C. Guo, Y. Wang, K. X. Song

**ABSTRACT.** Soil salinity and temperature are major factors that influence the dielectric properties of soil. To evaluate the effect of these factors on a soil moisture sensor based on dielectric properties, a loess soil sample from Shenmu County, Shaanxi Province, and a sandy soil sample from Dangshan County, Anhui Province, were tested. Two frequency domain reflectometry (FDR) sensors were employed to measure the output for different moisture contents (4.4%–22%), temperatures (5°C–50°C) and salinity levels (0%–1%). The results showed that the indicated moisture output increased with temperature and soil salinity (0%–0.4%), and was relatively stable with salinity (0.4%–1%). A mathematical model relating sensor output, moisture content, salinity, and temperature was established. This model can be used to develop FDR soil moisture sensor calibration equations with temperature and salinity compensation functions.

**Keywords.** Dielectric properties, FDR, Moisture content, Salinity, Soil, Temperature.

Soil moisture is an important physical parameter that significantly influences plant growth (Kampf and Tyler, 2005; Noble, 1997). Water is not only an essential substance for photosynthesis but also an indispensable constituent of the plant itself. To rapidly acquire soil moisture measurements, Topp et al. (1980) introduced the method of time domain reflectometry (TDR), and it has been widely used in recent years because of its rapid, accurate, and continuous measurement; however, the accuracy of TDR measurements of soil moisture depends on that of measurement time. On the other hand, frequency domain reflectometry (FDR) (Sun et al., 2010; Wojciech and Andrzej, 2010; Andrzej et al., 2012), which measures moisture content based on the effect of water on the dielectric properties of soil, has wider frequency and moisture measurement ranges, and its accuracy does not depend on that of measurement time. Furthermore, it is increasingly being used for monitoring soil moisture automatically and continuously (Ma, 2008).

Dielectric constant is a quantity used to describe the dielectric properties that influence the reflection of electromagnetic waves at interfaces and the attenuation of wave energy within materials (Feng et al., 2002). Numerous researchers have examined models relating dielectric constant to the moisture content of the soil (Herkelrath et al., 1991; Roth et al., 1992). In particular, the completely empirical equation proposed by Topp et al. (1980) and the semi-theoretical and semi-empirical equation proposed by Herkelrath et al. (1991) are widely used. The Topp formula depends only on the soil dielectric constant and is relatively independent of soil texture, bulk density, temperature, and soil salinity. The results of

applying the TDR technique to measure moisture content are encouraging (Topp et al., 1980). However, several subsequent studies have demonstrated that relatively large errors exist if the Topp equation is applied to different types of soils, thus this formula must be used through the use of an empirical correction equation (Robinson et al., 2003). The abovementioned semi-theoretical and semi-empirical equation proposed by Herkelrath et al. (1991) shows that within a particular soil moisture content range, soil moisture is linearly correlated with the square root of the dielectric constant. Jacobsen and Schjinning (1994) verified the applicability of the Herkelrath formula, but noted that empirical calibration parameters must be accurately determined for different soils before the formula is used. Therefore, it is necessary to study model parameters aimed at different types of soil.

Other researchers have studied typical Chinese soil types using the model. Zhu et al. (2011) examined four types of clay soil in China and studied the empirical relationships between dielectric constants and volumetric moisture contents to appropriately modify the Topp equation and determine the correction parameters of the Herkelrath equation for the examined soils. As for soil salinity, only microwave network measurements have been employed to examine how the dielectric constants for soil samples depends on frequency, salinity, and moisture content (Shao et al., 2002; Lei, 2011). However, FDR can measure soil dielectric properties more accurately than

---

Submitted for review in November 2013 as manuscript number SW 10499; approved for publication by the Soil & Water Division of ASABE in April 2014.

The authors are **Bei Liu**, Master of Science, College of Mechanical and Electronic Engineering, Northwest A&F University, Yangling China; **Wen Ting Han**, Professor, College of Mechanical and Electronic Engineering, Northwest A&F University; Institute of Water Saving Agriculture in Arid Areas of China, Northwest A&F University; Institute of Soil and Water Conservation, China Academy of Sciences & Ministry of Water Resources, Yangling, China; **Paul Weckler**, Professor, Oklahoma State University Stillwater, Oklahoma; **Wen Chuan Guo**, Professor, **Yi Wang**, Master of Science, **Ke Xin Song**, Master of Science, College of Mechanical and Electronic Engineering, Northwest A&F University, Yangling, China. **Corresponding author:** W. T. Han, No. 26, Xinong Road, Yangling, 712100, China; phone: +862987091325; e-mail: hanwt2000@126.com.

other techniques; therefore, we decided to measure the effect of temperature and salinity on FDR measurement.

Dielectric properties of materials are affected by several factors including the frequency of the measurement waves, temperature, and moisture content (Komarov et al., 2005). However, the effect of soil salinity on electronic transmission conditions has rarely been considered. At the same time, the parameters of existing soil moisture measurement model all without soil salinity, but because of soil itself contains kinds of salts according to the analysis of various soils texture, it is necessary to study the effect of salinity on dielectric properties. Moreover, there are many different types of soil, and sensors need to be recalibrated when a type of soil being monitored changes.

This study had two aims: 1) to study loess and sandy soil samples that were characteristic of typical Chinese soils using two types of FDR soil moisture sensors, and 2) to explore the effects of different soil salinities and soil temperatures on moisture measurements that are based on the dielectric properties of the loess and sandy soil samples, and to establish a model to measure moisture that provides a technical basis for the development of a soil moisture detector with temperature and salinity compensation functions.

## MATERIALS AND METHODS

Two characteristic Chinese soils were examined: loess soil and sandy soil. The loess soil sample was from Shenmu Shaanxi, Northwest China, 38°58'N, 110°30'E. Shenmu County is located in the northern part of Shaanxi Province in a zone of transition between loess hills and the grasslands of Inner Mongolia. The soil was from a jujube orchard in the hilly region of the Loess Plateau in northern Shaanxi. The sloped soil of the jujube orchard was significantly deficient in nitrogen (N) and phosphorus (P), but relatively rich in potassium (K).

The sandy soil sample was from Dangshan Anhui, East China, 34°16'N, 116°29'E. Dangshan County is located in the northernmost portion of Anhui Province. It is located in the alluvial plain of the Yellow River, which typically features sand soil (Dong, 2012). The samples were collected from a 40-year-old pear orchard in its senescent phase. The pear trees were mainly fertilized with organic fertilizers in combination with the administration of N, P, and K.

The output signals from two FDR soil moisture sensors, TM-100Y and DSW-T2, were measured for 50 samples with various moisture contents and salinities (as described in table 1) as a function of temperature. We then developed a model for the results using the Box-Behnken design (BBD; as described later in the section "Model Building Methods").

### PREPARATION OF SOIL SAMPLES

The soil samples were obtained from 20 to 30 cm below the surface to avoid surface disturbances and to obtain a stable soil structure, as suggested by Kampf and Tyler (2005). After small stones, weeds, and other impurities

were removed, the soil was allowed to dry under natural conditions. The soil samples were ground to powder and passed through an 80-mesh sieve (with a pore size of 0.2 mm). The resulting soil particles with diameters less than 0.2 mm were used in the experiment. Because two soil moisture sensors, TM-100Y and DSW-T2, were used to test each sample, two identical soil samples were prepared.

For this experiment, the bulk density of the soil samples were all set at 1.1 g cm<sup>-3</sup>, and the total volume of two containers used for the measurements was 500 mL; therefore, the required dry soil mass was 548 g according to the standard bulk density/volume formula. The initial average moisture content of the sandy and loess soil samples were 0.28% and 1.12%, respectively, and the initial average soluble salt content of the sandy and loess soil samples were 0.1018 and 0.0789 g kg<sup>-1</sup>, respectively. Five 600 g samples with initial moisture content levels were prepared for each type of soil that was tested. The final mass of the samples with different target moisture levels were calculated using equation 1:

$$M = 600 + m = 600 + 548 \times (m_{wl} - m_{w0}), \quad (1)$$

where  $M$  = final mass of target moisture level sample (g),  $m$  = mass of water added (g),  $m_{wl}$  = target moisture level (%), and  $m_{w0}$  = initial moisture content (%).

NaCl for weighted salinities (as compared with final mass of sample) of 0 wt%, 0.2 wt%, 0.4 wt%, 0.7 wt%, and 1 wt% was added to the required amount of water for each target moisture content and was allowed to dissolve. The resulting solutions were sprayed onto the appropriate soil samples and left to stand (Hu, 2003; Pu et al., 2012). The samples were then packaged into plastic bags and left to stand for 24 h to mix the water and salt with the soil as evenly as possible. The actual moisture content of samples were calculated by oven drying method. Three copies of soil, weighing 2 to 3g, were extracted from each test sample and dried in an oven at 105°C for 24 h. The average soil moisture of these three copies was used for the test sample moisture content. Finally, the 50 soil samples, prepared according to table 1, were stored at 2°C for 24 h before the FDR measurements.

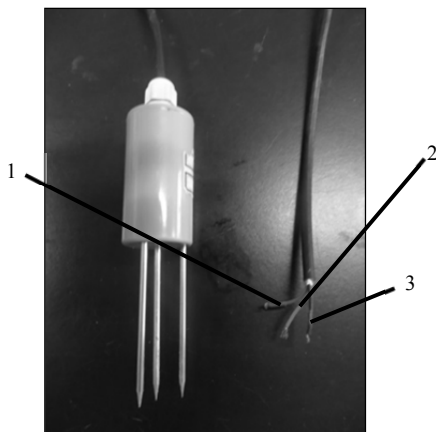
The moisture contents obtained by oven drying method and those measured using the soil moisture sensors were compared. The output of the DSW-T2 and TM-100Y sensors produced volumetric moisture data that were converted to gravimetric results by the standard bulk density/volume formula. All moisture content data discussed in the remainder of this paper refers to gravimetric moisture content. Ten sets of data were measured for each soil sample at 5°C intervals from 5°C to 50°C. Thus, 500 data points were obtained from each sensor.

### FDR SOIL MOISTURE SENSORS

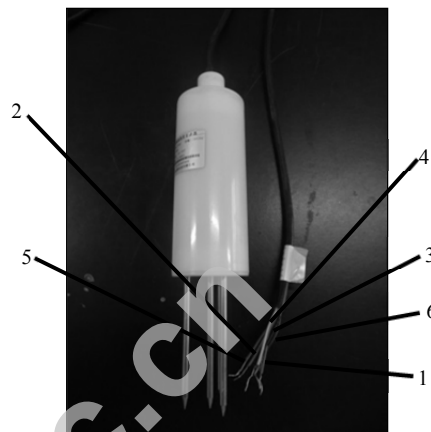
Two types of FDR soil moisture sensors were tested in this study, TM-100Y (Handan Yimeng, Handan, China) is shown in figure 1, and DSW-T2 (Beijing DiHui Technology, Beijing, China) is shown in figure 2. The technical parameters of the two soil moisture sensors are provided in appendix 1. Before the experiment, the two

**Table 1 Soil sample compositions.**

Sample 1: Sandy Soil from Dangshan, Anhui			Sample 2: Loess Soil from Shenmu, Shaanxi		
Moisture Content (%)	Amount of Added NaCl	Quantity	Moisture Content (%)	Amount of Added NaCl	Quantity
3.82		5	6.2		5
11	For each moisture content, 0%, 0.2%,	5	7.8	For each moisture content, 0%, 0.2%,	5
12.9	0.4%, 0.7%, or 1% NaCl for a total of	5	13	0.4%, 0.7%, or 1% NaCl for a total of	5
18.2	5 samples for each moisture content	5	16.9	5 samples for each moisture content	5
22.02		5	21.4		5
Total					50

**Figure 1. TM-100Y soil moisture sensor.**

The 1 and 3 wires are the power and ground connectors for the moisture measurement circuit. The 2 wire is the moisture content signal output port.

**Figure 2. DSW-T2 soil temperature and moisture sensor.**

The 1 and 3 wires are the power and ground connectors for the moisture measurement circuit. The 4 and 5 wires are the power and ground connectors for the temperature measurement circuit. The 6 and 2 wires are the signal output ports for moisture content and temperature.

sensors' probes were calibrated with air and 25°C deionized water. Then, the dielectric parameters of deionized water were measured at 25°C and compared with the known parameters. Before each test, the output voltage of the power supply was tested by a digital multimeter to ensure normal output, and the digital thermometer was zeroed by placing the probe in an ice-water mixture.

#### SYSTEM AND METHOD OF MEASURING SENSOR OUTPUT SIGNALS

##### *Experimental Principle*

The experimental system consists of thermostatic oven (YHG-400BS, Shanghai Yuejin Medical Instrument, temp. fluctuation:  $\pm 1^\circ\text{C}$ ), WD-5 regulated power supply (Qidong Simaite Computer Factory, China), DM6801 digital thermometer (Shenzhen Victor Hi-Tech, Co., China), multimeter (Shenzhen Victor Hi-Tech, Co., China), DSW-T2 and TM-100Y sensors (fig. 3). During the measurement, the DSW-T2 and TM-100Y sensors were inserted into the central portions of the two identical soil samples and then were put into the thermostatic oven to heat the samples to the set temperature. WD-5 regulated power supply was used to supply to the DSW-T2 and TM-100Y sensors. Finally, output signals from the two sensors could be measured by multimeter.

##### *Experimental Method*

Prior to the sensor measurements, a thermostatic oven was set to a temperature of 5°C. Two soil samples were

removed from the freezer and placed in the drying oven for 12 h. The DSW-T2 and TM-100Y sensors were inserted into the central portions of the two identical soil samples while they were in the oven, and a DM6801 digital thermometer was inserted into each of the soil samples. When the temperature of the soil sample stayed constant at 5°C for 3 min, output signals from the two sensors were measured by multimeter. WD-5 regulated power supply was used to supply 12 and 9 V to the DSW-T2 and TM-100Y sensors, respectively. This method was repeated for each drying oven temperature at 5°C intervals for a total range of 5°C to 50°C. Throughout the process, the soil samples were covered with plastic wrap to prevent water loss due to heat-induced evaporation. The measurement system is shown in figure 3, and a schematic diagram of the measurement system is presented in figure 4.

#### MODEL BUILDING METHODS

Response surface methodology uses regression methods to establish algorithms that use polynomial approximations to estimate experimental conditions and results of multi-factor tests, allowing constraints and experimental results to be expressed in terms of functions. An intuitive surface can then be formed in a three-dimensional coordinate plane to quantitatively observe the effects of each factor on the experimental results (Sun, 2002; Velazquez-Martí et al., 2005; Zhang et al., 2011). Specifically in this study, the BBD was utilized to build variance models through response surface methodology. The BBD box plot design involves a class of rotatable or nearly rotatable second-



Figure 3. Pictures of the experimental system for measuring the output of the DSW-T2 and TM-100Y soil sensors.

order designs based on three-level incomplete factorial designs (Edwards and Mee, 2010).

## RESULTS AND ANALYSIS

### DEPENDENCE OF MOISTURE SENSOR MEASUREMENTS ON TEMPERATURE FOR PARTICULAR SALINITIES

The dependence of the output voltage of the TM-100Y on temperature at different NaCl concentrations for (a) sandy and (b) loess soils with initial moisture contents of 3.82% and 6.2%, respectively, are shown in figure 5. This figure indicates that the TM-100Y output voltage gradually increased with increasing temperature.

The dependence of the output current of the DSW-T2 on temperature for different NaCl concentrations for (a) sandy and (b) loess soils with initial moisture contents of 3.82% and 6.2%, respectively, are shown in figure 6. This figure reveals that the output current of the DSW-T2 gradually increased with increasing temperature. The same phenomenon was also observed for soil samples with different moisture contents.

Because the dielectric constant of water in soil pores changes with temperature, the dielectric constant of soil also varies with temperature. In addition, the dielectric properties of soil represents molecular polarizability in the electrostatic field and dynamic equilibria among Brownian motion. Increasing temperature can enhance the polarization of molecules and can increase the Brownian motion of the ionic solution surrounding the soil particles, leading to an increase in dielectric constants, which we measure as an increase in output from the sensors. Figures 5 and 6 show that temperature is a major factor affecting the output of FDR sensors.

### DEPENDENCE OF MOISTURE SENSOR MEASUREMENTS ON SALINITY

#### At Different Temperatures

The dependence of the output voltage of the TM-100Y sensor on salinity for (a) sandy and (b) loess soils with moisture contents of 11% and 13%, respectively, at different temperatures are shown in figure 7. This figure indicates that, on the whole, the TM-100Y output voltage increased with increasing salinity. In particular, the output voltage tended to increase with increasing salinity when salinity was between 0% and 0.4%, but it declined with increasing salinity when salinity was between 0.4% and 1%. A maximum output voltage was observed at a salinity of 0.4%. This phenomenon was also observed for soil samples with different moisture contents.

The dependence of the output currents of the DSW-T2 on salinity at different temperatures for (a) loess and (b) sandy soils with initial moisture contents of 6.2% and 11%, respectively, are shown in figure 8. This figure indicates that, on the whole, the output voltage of the DSW-T2 increases with increasing salinity. In particular, the output voltage tended to increase with increasing salinity when salinity was between 0% and 0.4%, but tended to decrease with increasing salinity when salinity was between 0.4% and 1%. Maximum output voltages were observed for salinities from 0.4% to 0.7%. This phenomenon was also observed in soil samples with different moisture contents.

#### At Different Moisture Content Levels

The dependence of the output voltage of the TM-100Y on salinity at different moisture content levels for (a) sandy and (b) loess soils at 25°C and 15°C, respectively, are shown in

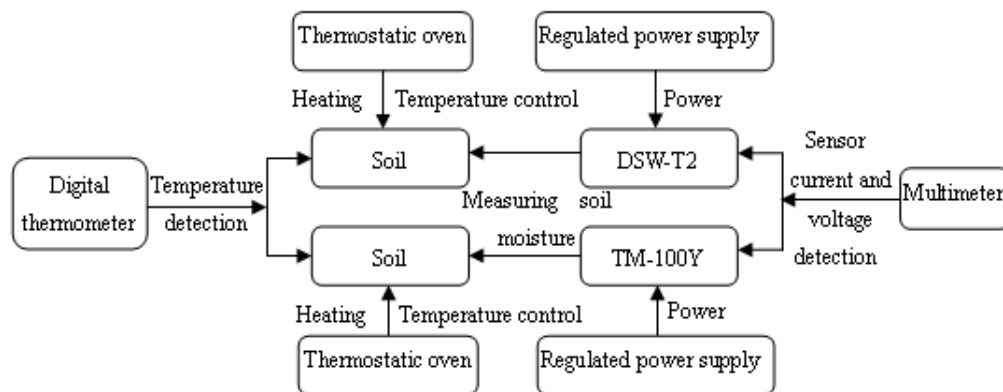


Figure 4. Schematic diagram for measuring the outputs of the DSW-T2 and TM-100Y soil sensors.

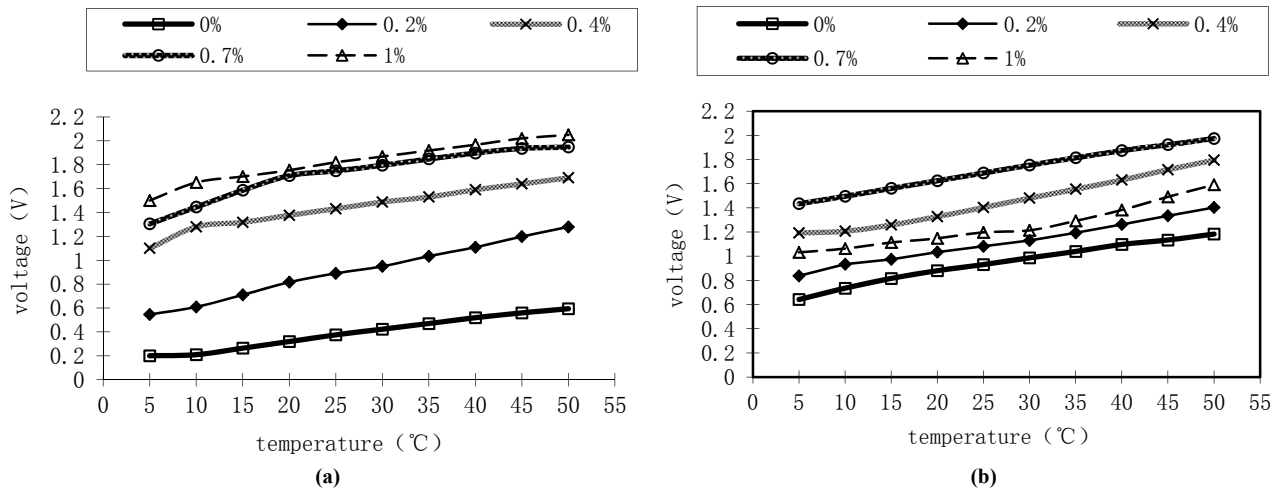


Figure 5. Dependence of the output voltage of the TM-100Y on temperature for sandy (a) and loess (b) soils with initial moisture contents of 3.82% and 6.2%, respectively, for different NaCl concentrations.

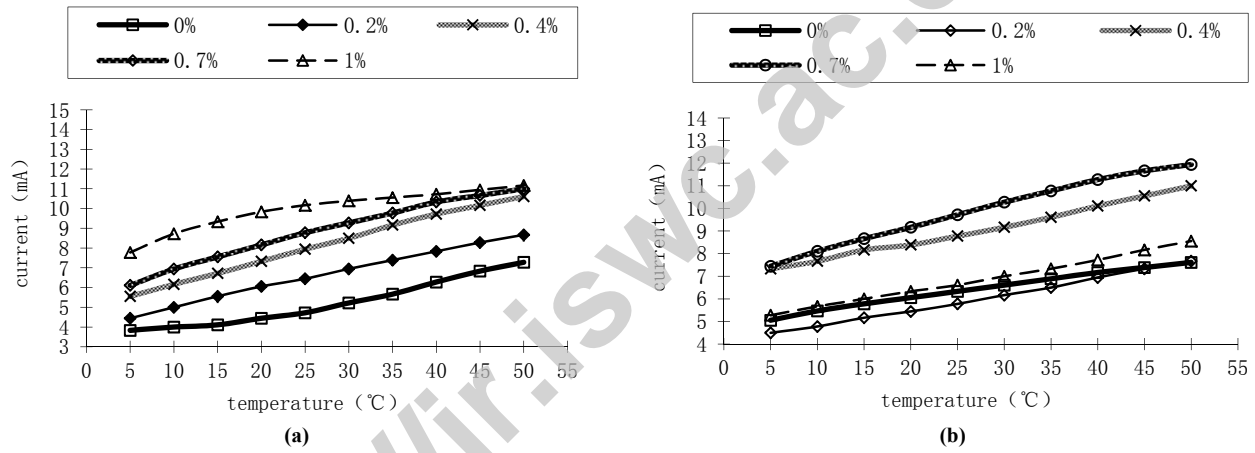


Figure 6. Dependence of the output current of the DSW-T2 on temperature for sandy (a) and loess (b) soils with initial moisture contents of 3.82% and 6.2%, respectively, for different NaCl concentrations.

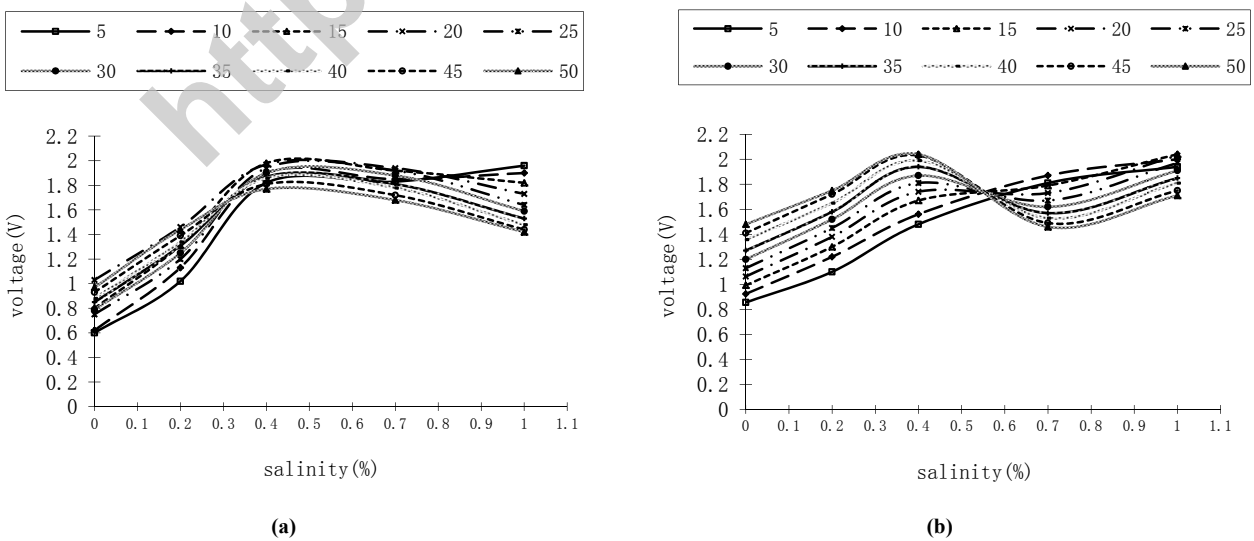
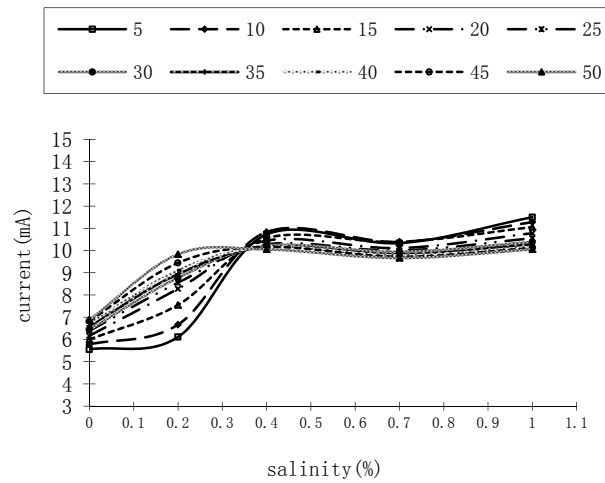
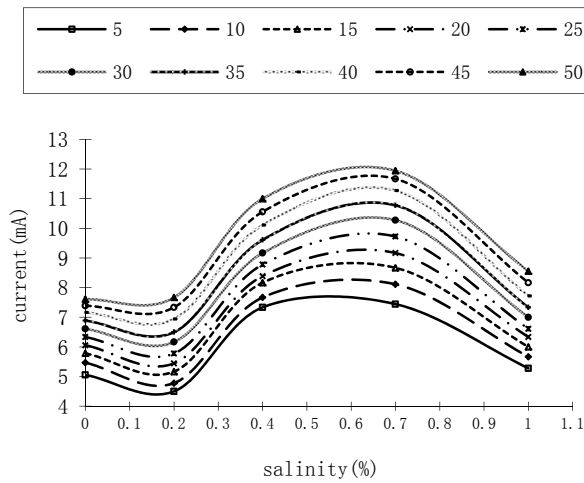


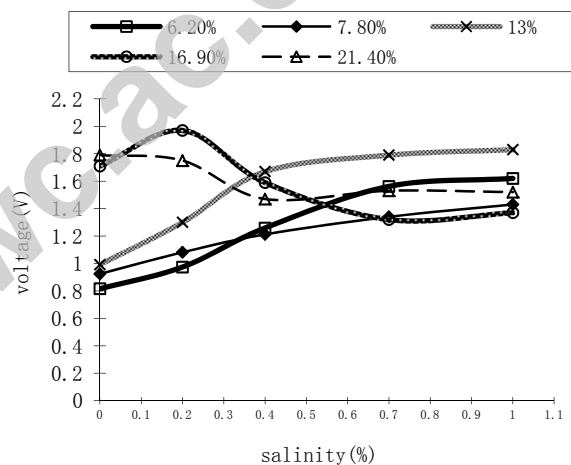
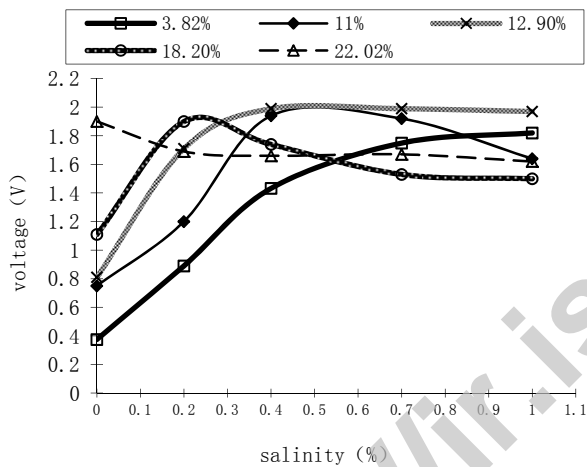
Figure 7. Dependence of the output voltage of the TM-100Y on salinity for sandy (a) and loess (b) soils with initial moisture contents of 11% and 13%, respectively, at different temperatures.



(a)

(b)

Figure 8. Dependence of the output current of the DSW-T2 on salinity for loess (a) and sandy (b) soils with initial moisture contents of 6.2% and 11%, respectively, at different temperatures.



(a)

(b)

Figure 9. Dependence of the output voltage of the TM-100Y on salinity for sandy (a) and loess (b) soils at 25°C and 15°C, respectively, at different moisture content levels.

figure 9. The dependence of the output current of the DSW-T2 sensor on salinity for different moisture content levels for (a) loess and (b) sandy soils at 45°C and 35°C, respectively, are shown in figure 10. Figures 9 and 10 reveal that moisture content significantly affected output signals when salinity was between 0% and 0.4%, but that these effects gradually decreased when salinity was between 0.4% and 0.7%. Moisture content had no significant effects on the output signals of the sensors when the salinity was between 0.7% and 1%.

The dielectric properties of soil are affected by salinity, texture, moisture content, and other characteristics of the soil. Soil salinity and the concentration of ions in soil solutions are positively correlated. The concentration of ions in soil solutions is difficult to measure; therefore, *in situ* experiments are usually performed to obtain values for soil salinity. However, electromagnetic waves are affected more strongly by ion concentrations in soil solutions rather than soil salinity. When the salinity of the soil is relatively

low, soils with different moisture levels will have soil solutions with significantly different ion concentrations, resulting in large differences in dielectric properties. Consequently, differences in moisture level will significantly impact the output signal for low salinities. When the salinity of the soil is relatively high, variation in the moisture content in unsaturated soil samples will cause only small differences in ion concentrations in soil solutions. This will produce only small differences in soil dielectric properties and will therefore cause less significant changes in moisture sensor output signals. Figures 7 to 10 demonstrate that soil salinity affects the output signals of FDR soil moisture sensors; thus, the effect of salinity on dependence of output signals must be considered when measuring soil moisture with great accuracy.

Figure 11 depicts the responses of (a) the output voltage of the TM-100Y and (b) the output current of the DSW-T2 to temperature and salinity for loess (a) and sandy (b) soils

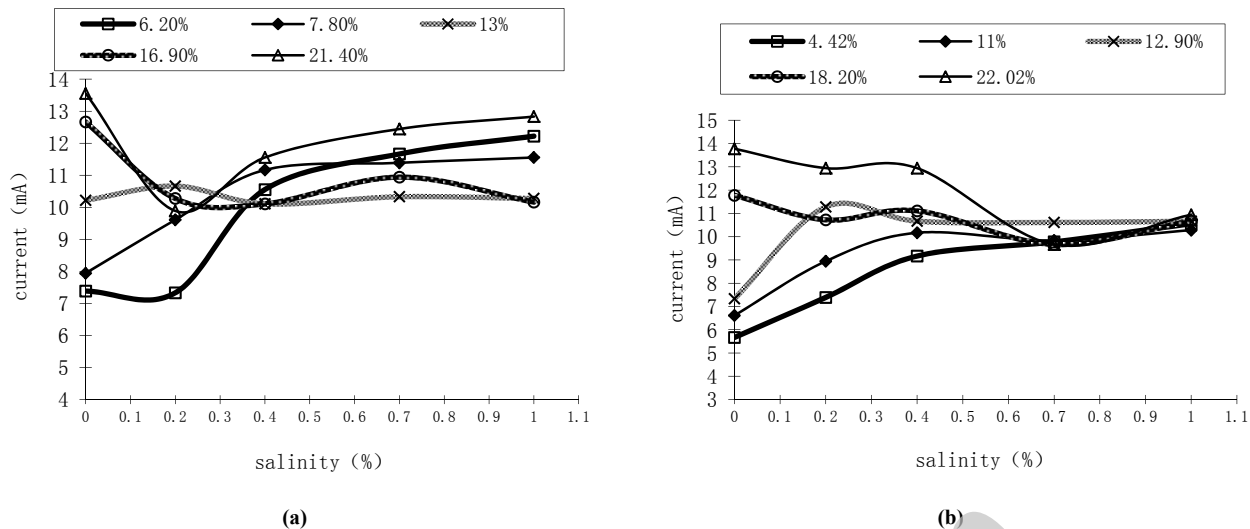


Figure 10. Dependence of the output currents of the DSW-T2 on salinity for loess (a) and sandy (b) soils at 45°C and 35°C, respectively, at different moisture content levels.

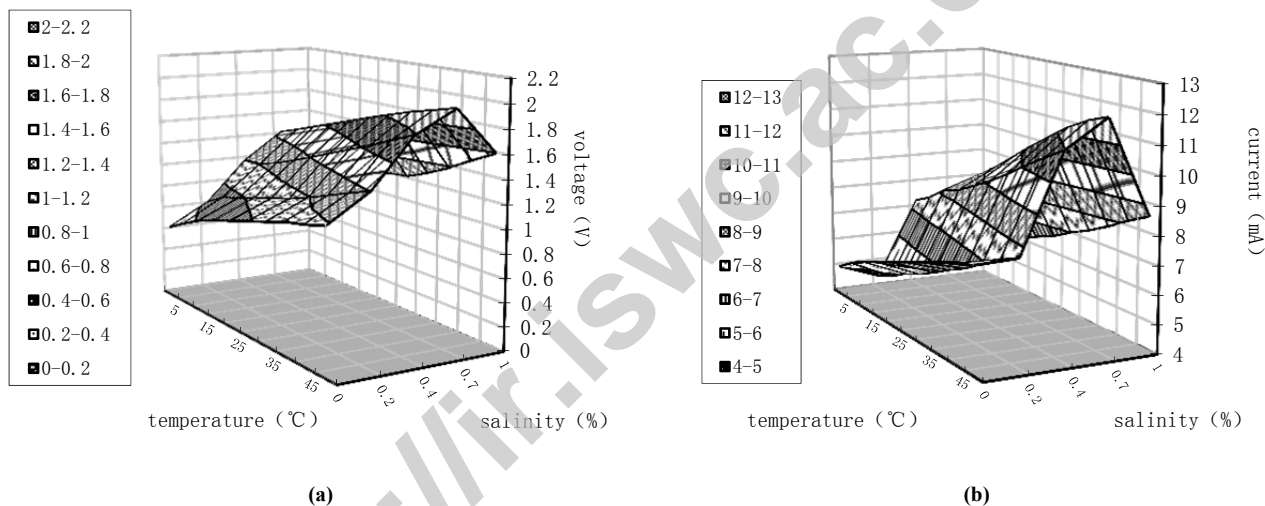


Figure 11. Response surfaces of the output voltage of (a) the TM-100Y and (b) the output current of the DSW-T2 to temperature and salinity changes for loess (a) and sandy (b) soils with a moisture content of 6.2%.

with a moisture content of 6.2%. This figure indicates that the output voltage of the TM-100Y increased with increasing temperature, though this voltage was initially observed to increase and subsequently decrease as salinity increased. The output current of the DSW-T2 increased with increasing temperature, and initially increased and subsequently decreased with increasing salinity.

#### DEVELOPMENT OF THE MEASUREMENT MODEL

A total of 500 datasets were obtained for each of the sensors. For each sensor, 250 datasets were uniformly selected from these 500 datasets and subjected to multivariate regression using Design-Expert 8.0 software (Stat-Ease, Inc., Minneapolis, Minnesota, USA).

The fitted equation for the TM-100Y soil moisture sensor is provided by equation 2:

$$U = -0.387 + 0.117m_w + 3.71Y + 0.0165T - 0.0996m_wY - 8.23 \times 10^{-4}m_wT - 6.88 \times 10^{-3}YT - 1.06 \times 10^{-3}m_w^2 - 1.64Y^2 - 2.05 \times 10^{-5}T^2 \quad (2)$$

where  $U$  = output voltage of the moisture sensor (V),  $m_w$  = gravimetric moisture content of the sample (%),  $Y$  = salinity of the sample (%), and  $T$  = sample temperature (°C).

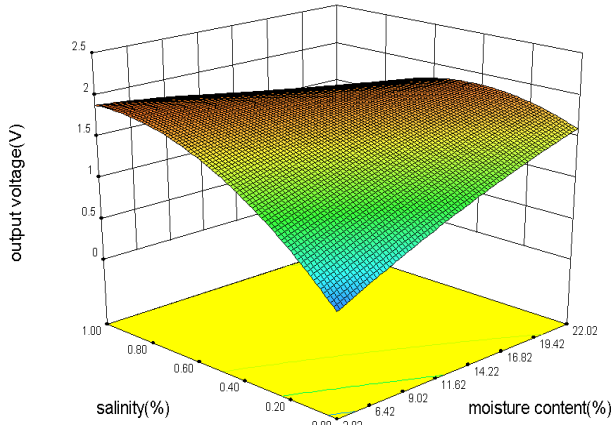
Analyses of variance were performed using equation 2, and the results of these analyses are provided in table 2.

Table 2 demonstrates that the P-value for equation 2 was less than 0.0001, indicating that the model is highly significant. The coefficient of determination of the model was  $R^2 = 0.7492$ , suggesting that the output voltage of the sensor and the temperature, moisture content, and salinity of the soil sample were highly correlated. Moreover, with the exception of  $YT$ ,  $T$ , and  $T^2$ , the remaining terms in equation 2 exhibited highly significant effects. The

**Table 2. Analysis of variance for the regression model described by equation 2.**

Source of Variance	Sum of Squares	Degrees of Freedom	Mean Square	F-value	P-value	Significance <sup>[a]</sup>
$m_w$	2.74	1	2.74	58.09	< 0.0001	**
$Y$	10.75	1	10.75	228.35	< 0.0001	**
$T$	0.082	1	0.082	1.75	0.1869	
$Y m_w$	12.23	1	12.23	259.67	< 0.0001	**
$T m_w$	1.36	1	1.36	28.91	< 0.0001	**
$YT$	0.31	1	0.31	6.56	0.0110	
$m_w^2$	0.38	1	0.38	8.10	0.0048	
$Y^2$	7.12	1	7.12	151.22	< 0.0001	**
$T^2$	3.460E-003	1	3.460E-003	0.073	0.7866	
Model	33.76	9	3.75	79.65	< 0.0001	**
Error	11.30	240	0.047			
Total	45.06	249				

<sup>[a]</sup> \*\*  $P \leq 0.01$ ; highly significant.



**Figure 12. Response surface indicating the effects of sample salinity and moisture content on the output voltage of the TM-100Y at 26.25°C.**

response surface for equation 2 at 27.5°C is illustrated in figure 12.

The fitted equation for the DSW-T2 soil moisture sensor is described by equation 3:

$$\begin{aligned}
 I = & 0.678 + 0.509m_w + 4.19Y + 0.16T \\
 & - 0.178m_w Y - 5.40 \times 10^{-3} m_w T - 0.0105YT \\
 & - 6.58 \times 10^{-4} m_w^2 - 0.382Y^2 - 6.02 \times 10^{-4} T^2
 \end{aligned} \quad (3)$$

where  $I$  = output current of the moisture sensor (mA),  $m_w$  = gravimetric moisture content of the sample (%),  $Y$  = salinity of the sample (%),  $T$  = sample temperature (°C)

Analyses of variance were performed for equation 3, and the results of these analyses are provided in table 3.

Table 3 illustrates that equation 3 has a P-value of less than 0.0001, indicating that the model is highly significant. The coefficient of determination of the model was  $R^2 = 0.7146$ , suggesting that the output current of the sensor was highly correlated with sample temperature, moisture content, and salinity. Moreover, with the exception of  $m_w^2$ ,  $YT$ ,  $Y^2$ , and  $T^2$ , the remaining variables in equation 3 exhibited highly significant effects. The response surface of equation 3 at 10.47°C is depicted in figure 13.

### MODEL VARIATION

The output signals of the two sensors were measured for the remaining 250 datasets at three to four arbitrary temperatures between 5°C and 50°C. To obtain calculated output signals, we wrote programs using Matlab 2010b software (Mathworks Company, Natick, Mass.) based on the models described by equations 2 and 3, where the moisture contents, temperatures, and salinities are the variables. Then, the calculated output was compared with the measured data of one of the soil samples, as shown in figure 14. The calculated values and the measured data are closely distributed on both sides of the 45° line, with  $R^2 = 0.905$  and  $R^2 = 0.919$  for models 2 and 3, respectively. Therefore, models 2 and 3 can be used to calibrate the output voltage signals of the sensors with good accuracy.

This experiment established an FDR soil moisture detection model for Chinese loess and sandy soils, and we validated the model using the new 250 datasets with a high degree of correlation. This model can be used to calibrate FDR

**Table 3. Analysis of variance for the regression model described by equation 3.**

Source of Variance	Sum of Squares	Degrees of Freedom	Mean Square	F-value	P-value	Significance <sup>[a]</sup>
$m_w$	498.57	1	498.57	369.99	< 0.0001	**
$Y$	35.17	1	35.17	26.10	< 0.0001	**
$T$	114.51	1	114.51	84.98	< 0.0001	**
$Y m_w$	31.91	1	31.91	23.68	< 0.0001	**
$T m_w$	47.80	1	47.80	35.47	< 0.0001	**
$YT$	0.72	1	0.72	0.53	0.4660	
$m_w^2$	0.061	1	0.061	0.045	0.8322	
$Y^2$	0.39	1	0.39	0.29	0.5934	
$T^2$	2.99	1	2.99	2.22	0.1374	
Model	809.71	9	89.97	66.77	< 0.0001	**
Error	323.40	240	1.35			
Total	1133.11	249				

<sup>[a]</sup> \*\*  $P \leq 0.01$ ; highly significant.



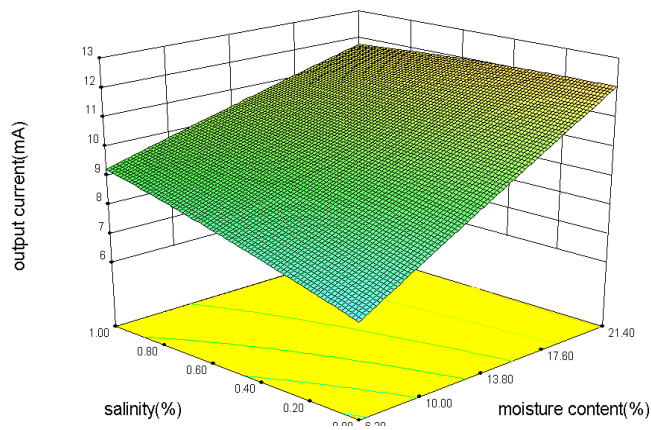


Figure 13. Response surface indicating the effects of sample salinity and moisture content on the output current of the DSW-T2 at 10.47°C.

moisture measurements for some types of Chinese soil, and as a reference for future researchers analyzing other soil types.

## CONCLUSIONS

In this study, moisture content of the loess soil from Shenmu, Shaanxi, and the sandy soil from Dangshan, Anhui, were measured. The output signals of two FDR-based soil moisture sensors were measured for samples with different moisture contents, temperatures, and salinities. Based on our experiments, we draw the following conclusions:

1. Soil salinity significantly impacted the output of the FDR soil moisture sensors when the salinity was lower than 0.4%; the measured results increased with increasing salinity. Changes in salinity had little impact on these measurements when the salinity was between 0.4% and 1%.
2. Temperature significantly impacted the output of the FDR soil moisture sensors. In particular, the measured moisture content increased with increasing temperature.
3. Calibration models were established for both the TM-100Y and DSW-T2 sensors that related output signals to the actual moisture content, temperature, and salinity of the tested soil. The coefficients of determination for the two models were  $R^2 = 0.7492$  and  $R^2 = 0.7146$ .

= 0.7146, suggesting that the output signals of the two sensors were highly correlated with the sample temperature, moisture content, and salinity. The P-values for the two equations were less than 0.0001, indicating that the two models were highly significant. These models can provide guidance for designing FDR-based soil moisture sensors with temperature and salinity compensation functions.

In addition, this research has raised several additional questions that require further study:

- The relationship between soil salinity and ionic concentrations (salinity of the soil solution) is not sufficiently clear; thus, further analyses of salt dissolution, deposition, ion activity, pressure, chemical equilibrium, and other factors are required to elucidate this relationship.
- In this study, NaCl was utilized to study soil salinity. Although NaCl is the salt present in a majority of salinized soils in nature, other widely distributed salts also exist. These salts might have calibration parameters that differ from those of NaCl.

## ACKNOWLEDGEMENTS

This article was funded by the Supported by Program for New Century Excellent Talents in University (NCET-12-0473), the National Science & Technology Supporting Plan (2011BAD29B08) and the Science and Technology Innovation Project from Northwest A&F University (Z109021202).

## REFERENCES

- Andrzej, W., Agnieszka, S., Wojciech, S., Jolanta, C., Viliam, P., & Grzegorz, J. (2012). Determination of soil pore water salinity using an FDR sensor working at various frequencies up to 500 MHz. *Sensors*, 12(8), 10890-10905. doi:http://dx.doi.org/10.3390/s120810890
- Dong, S. Y. (2012). Dangshan pear soil testing and fertilizer formulation technology. *Anhui Agric. Sci. Bull.*, 18(4), 59-61.
- Edwards, D. J., & Mee, R. W. (2010). Fractional box-Behnken designs. *J. Quality Tech.*, 43(4), 1-31.
- Feng, H., Tang, J., & Cavalieri, R. P. (2002). Dielectric properties of dehydrated apples as affected by moisture and temperature. *Trans. ASAE*, 45(1), 129-135. doi:http://dx.doi.org/10.13031/2013.7855

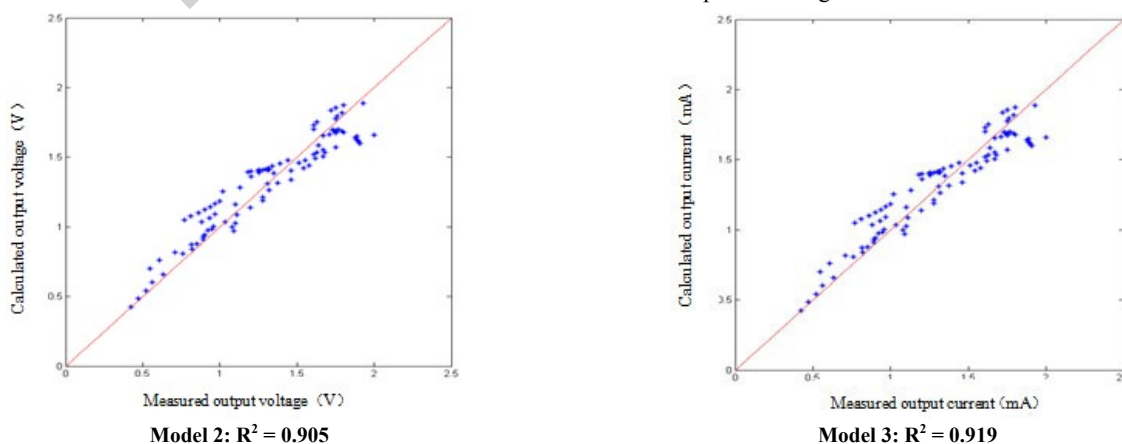


Figure 14. Calculated output against measured output of soil samples.

- Herkelrath, W. N., Hamburg, S. P., & Murphy, F. (1991). Automatic, real-time monitoring of soil moisture in a remote field area with time domain reflectometry. *Water Resour. Res.*, 27(5), 857-864. doi:http://dx.doi.org/10.1029/91WR00311
- Hu, Q. R. (2003). Studies on microwave dielectric behavior of moist salt soil and its effect on backscattering coefficients extracted from radar image. PhD diss. Beijing, China: Chinese Academy of Sciences, Institute of Remote Sensing Applications.
- Jacobsen, O. H., & Schjinning, P. (1994). Comparison of TDR calibration functions for soil water determination. *Proc. Time Domain Reflectometry, Applications in Soil Science*, 9-23. Aarhus, Denmark: Denmark Research Centre Foulum.
- Kampf, S. K., & Tyler, S. W. (2005). Evaporation and land surface energy budget at Salarde Atacama, Northern Chile. *J. Hydrology*, 310(1-4), 236-252. doi:http://dx.doi.org/10.1016/j.jhydrol.2005.01.005
- Komarov, V., Wang, S., & Tang, J. (2005). Permittivity and measurement. In K. Chang (Ed.), *Encyclopedia of RF and Microwave Engineering*. Wiley Online: . doi:http://dx.doi.org/10.1002/0471654507.emc308
- Lei, L. (2011). Studies on the dielectric behavior of saline soil and its effect on backscattering coefficients extracted from radar images. PhD diss. Urumqi, Xinjiang Uyghur Autonomous Region, China: Xinjiang University.
- Ma, T. (2008). An analysis of rapid measuring technique on soil water at home and abroad. *China Flood Drought Mgmt.*, 2(1), 31-33.
- Noble, P. S. (1997). Root distribution and seasonal production in the north-western Sonaran Desert for a C3 shrub, a C4 bunchgrass and a CAM leaf succulent. *Amer. J. Crop Bot.*, 84(8), 949-945. doi:http://dx.doi.org/10.2307/2446285
- Pu, Z., Yu, R. D., Yin, C. Y., & Lu, Y. N. (2012). Optimal hyperspectral indices for soil salt content estimation on typical saline soil in arid areas. *Bull. Soil Water Cons.*, 32(6), 129-133.
- Robinson, D. A., Jones, S. B., Wraith, J. M., Or, D., & Friedman, S. P. (2003). A review of advances in dielectric and electric conductivity measurements using time domain reflectometry. *Vadose Zone J.*, 2(4), 444-475. doi:http://dx.doi.org/10.2136/vzj2003.4440
- Roth, C. H., Malicki, M. A., & Plagge, R. (1992). Empirical evaluation of the relationship between soil dielectric constant and volumetric water content as the basis for calibrating soil moisture measurements by TDR. *J. Soil Sci.*, 43(1), 1-13. doi:http://dx.doi.org/10.1111/j.1365-2389.1992.tb00115.x
- Shao, Y., Lu, Y., Dong, Q., & Han, C. M. (2002). Study on soil microwave dielectric characteristic as salinity and water content. *J. Remote Sensing-Beijing*, 6(6), 423-428.
- Sun, Y. R. (2002). Theoretical and experimental approach to the calculation of the impedance of soil probe. *Acta Pedologica Sinica*, 39(1), 120-126.
- Sun, Y., Ren, S., Ren, T., & Minasny, B. (2010). A combined frequency domain and tensiometer sensor for determining soil water characteristic curves. *Soil Sci. Soc. Amer. J.*, 74(2), 492-494. doi:http://dx.doi.org/10.2136/sssaj2009.0047N
- Topp, G. C., Davis, J. L., & Annan, A. P. (1980). Electromagnetic determination of soil water content measurement in coaxial transmission lines. *Water Resour. Res.*, 16(3), 574-582. doi:http://dx.doi.org/10.1029/WR016i003p00574
- Velazquez-Marti, B., Gracia-Lopez, C., & Plaza-Gonzalez, P. J. (2005). Determination of dielectric properties of agricultural soil. *Biosystems Eng.*, 91(1), 119-125. doi:http://dx.doi.org/10.1016/j.biosystemseng.2005.02.004
- Wojciech, S., & Andrzej, W. (2010). A FDR sensor for measuring complex soil dielectric permittivity in the 10-500MHz frequency range. *Sensors*, 10(4), 3314-3329. doi:http://dx.doi.org/10.3390/s100403314
- Zhang, L. F., Guo, W. C., Fu, H. X., & Xia, W. B. (2011). Designs for a digital honey water content meter. *Trans. Chinese Soc. Agric. Machinery*, 42(4), 139-143, 147.
- Zhu, A. N., Ji, L. Q., & Zhang, J. B. (2011). Empirical relationship between soil dielectric constant and colometric water content in various soils. *Acta Pedologica Sinica*, 48(2), 263-268.

## APPENDIX

**Table A1. Technical parameters of the TM-100Y soil moisture sensor.**

Specification	Parameter
Power supply	7-24 V (wide range of power supply voltage types, typically 12 V)
Measurement range	0-100% (with higher accuracy from 10 to 90%)
Accuracy	±3%
Probe length	60 mm
Probe diameter	3 mm
Probe material	Stainless steel (electrolysis resistant)
Sealing material	Black UV weathering-resistant ABS + epoxy resin (black, flame-retardant)
Response time	Less than 1 s
Output current	0-2 V
Product appearance operating	220 × 48 × 48 mm
Temperature	-45 to 80°C
Measurement area	A cylinder 7 cm in diameter and height centered on the central probe, with 95% of the effect derived from a cylinder 3 cm in diameter and 7 cm in height around the central probe.

**Table A2. Technical parameters of the DSW-T2 soil temperature and moisture sensor.**

Specification	Parameter
Power supply	18-24 V direct current
Measurement range	0-100% (moisture content), -30 to 70°C (temperature)
Accuracy	±3% (0-50%, moisture content) ±0.5°C (temperature)
Probe length	78 mm
Probe diameter	4 mm
Probe material	Stainless steel
Sealing material	ABS plastic
Response time	Less than 1 s
Output current	4-20 mA
Product appearance operating	220 × 48 × 48 mm
Work environment	Temperature of -30°C to 70°C, humidity of 0%-100% RH
Measurement area	A cylinder 7 cm in height and 3 cm in diameter centered on the central probe